Ferredoxin-NADP+ Oxidoreductase and Flavodoxin

Subjects: Biochemistry & Molecular Biology

Contributor: Takashi Iyanagi

Distinct isoforms of FAD-containing ferredoxin-NADP$^+$ oxidoreductase (FNR) and ferredoxin (Fd) are involved in photosynthetic and non-photosynthetic electron transfer systems. The FNR (FAD)-Fd [2Fe-2S] redox pair complex switches between one- and two-electron transfer reactions in steps involving FAD semiquinone intermediates. In cyanobacteria and some algae, one-electron carrier Fd serves as a substitute for low-potential FMN-containing flavodoxin (Fld) during growth under low-iron conditions. This complex evolves into the covalent FNR (FAD)-Fld (FMN) pair, which participates in a wide variety of NAD(P)H-dependent metabolic pathways as an electron donor, including bacterial sulfite reductase, cytochrome P450 BM3, plant or mammalian cytochrome P450 reductase and nitric oxide synthase isoforms. These electron transfer systems share the conserved Ser-Glu/Asp pair in the active site of the FAD module. In addition to physiological electron acceptors, the NAD(P)H-dependent diflavin reductase family catalyzes a one-electron reduction of artificial electron acceptors such as quinone-containing anticancer drugs. Conversely, NAD(P)H: quinone oxidoreductase (NQO1), which shares a Fld-like active site, functions as a typical two-electron transfer antioxidant enzyme, and the NQO1 and UDP-glucuronosyltransfease/sulfotransferase pairs function as an antioxidant detoxification system.

ferredoxin-NADP+ oxidoreductase (FNR) ferredoxin (Fd) flavodoxin (Fld) diflavin reductase family catalytic cycle electron transfer redox potentials evolutionary aspects

1. Introduction

Land plant and cyanobacterium ferredoxin (flavodoxin)-NADP$^+$ oxidoreductases (FNRs) catalyze the reversible electron transfer that occurs in the photosynthetic reaction (formation of NADPH) and non-photosynthetic reactions (NADPH-dependent redox metabolic pathways) (Equation (1)) [1][2][3][4][5][6]. The forward and reverse reactions of Equation (1) are catalyzed by distinct FNR and ferredoxin (Fd) isoforms [7]:

$$2\text{Fd}\ (\text{Fe}^{2+}) + \text{NADP}^+ + \text{H}^+ \rightleftharpoons 2\text{Fd}\ (\text{Fe}^{3+}) + \text{NADPH}\ (1)$$

In cyanobacteria and some algae, FMN-containing flavodoxin (Fld) acts as a one-electron carrier instead of ferredoxin (Fd) under iron-limiting conditions [8]. Meanwhile, the FNR- and Fld-like domains are present in eukaryotic NAD(P)H-dependent enzymes, including cytochrome P450 reductase (cyt P450 reductase) [9][10] and nitric oxide synthase (NOS) isoforms [11]. The catalytic domains of these enzymes share a high sequence similarity

and structure with FNR and Fld, where the FAD-FMN redox pair donates electrons to final electron acceptors during sequential one-electron transfer reactions [12]. NADH-cytochrome b_5 reductase (cyt b_5 reductase) shares structural similarities with plant FNR, despite its amino acid sequence similarities being lower [13]. The cyt b_5 reductase-cyt b_5 complex pair donates an electron to metal-containing proteins [14]. Cyt P450 reductase (FAD-FMN) and the cyt b_5 reductase (FAD)-cyt b_5 complex exhibit diverse functions in regard to the electron acceptors.

In addition to plant FNR, cyt P450 reductase and NOS isoforms catalyze a one-electron reduction of artificial electron acceptors such as quinone derivatives, where the resulting quinone radical reacts with molecular oxygen to form the superoxide radical [15][16][17][18][19], while NAD(P)H: quinone oxidoreductase (NQO1) bears a common flavodoxin-like topology in its active site [20] and catalyzes the two-electron reduction of anticancer quinone derivatives; the resulting hydroquinone form is primarily conjugated by UDP-glucuronosyltransferase (UGT) and sulfotransferase (SULT) [21]. Thus, the NQO1-UGT/SULT pair systems function as potent antioxidant enzyme systems.

2. Structure and Properties of the FNR, Fd and Fld

The three-dimensional structure of FNR from spinach reveals two subdomains, the NADPH-binding domain and the FAD-binding domain [1][5]. FNR can transfer electrons to both Fd [2Fe-2S] and Fld (FMN), where an interaction with Fd or Fld occurs in the same structural region of the FAD-binding domain [1][22]. Both Fd and Fld act as one-electron acceptors or donors, and Fd is replaced with Fld under low-iron conditions [8][23]. The rate of electron transfer among these proteins is controlled by several factors, including the relative orientation and distance between protein–protein interactions and the differences in the redox potentials between the protein-bound donor and acceptor redox cofactors [1][3][23][24][25][26]. Sinohara et al. [1] reported the crystal structures of the *R*FNR-*R*Fd (Fd III) (*R* for root) and *L*FNR-*L*Fd (Fd I) (*L* for leaf) complexes, and this provides a structural basis for reversing the redox pathway. In the *L*FNR-Fd complexes, the distance between the [2Fe-2S] cluster of Fd and the dimethylbenzene edge of the FAD ring is ~5.5–6.0 Å [1][24], while the *R*FNR-Fd complexes can utilize the different sides of the [2Fe-2S] cluster for intermolecular electron transfer. The modeling of the FNR-Fld complexes indicates that the distance between the two flavin rings is ~4.1 Å and that no intervening residues are present between the two cofactors, thus making possible direct one-electron transfer [25]. Taken together, these observations suggest that the complexes between oxidized FNR and oxidized Fd are relatively stable, as the complexes are stabilized by a salt bridge of FNR33Lys-Fd60Asp between FNR and Fd [26]. However, this stability is decreased by NADP(H) binding, and unstable complexes can promote the electron transfer rate during the catalytic cycle [27]. FNR interacts with Fd or Fld in photosynthetic and non-photosynthetic reactions.

The isoalloxazine ring of FAD in the leaf and root FNR is sandwiched between two aromatic residues (Tyr314 and Tyr95), where the phenol ring of carboxyl(C)-terminal Tyr314 shields the face of the isoalloxazine ring of FAD [5][28]. Thus, C-terminal Tyr314 must move away for productive hydride transfer from reduced FAD to $NADP^+$, and Ser96 interacts with the N5 atom of the isoalloxazine ring of FAD, where Ser96 forms a hydrogen bond with Glu312. Additionally, C-terminal Tyr314 and the Ser96-Glu312 pair modulates the affinity for $NADP^+$, the stabilization of

FAD semiquinone and the rate of electron transfer [29]. Therefore, Tyr314 and the Ser96-Glu312 pair are involved in the modulating of the flavin redox properties [30][31].

The formation of the reduced FAD-NADP$^+$ ($FADH^-$-$NADP^+$) complex with the charge transfer bands of 500–750 nm proceeds via an FAD_{ox}-NADPH charge-transfer species [32]. In the presence of excess NADPH (>10-fold), bound $NADP^+$ is replaced by NADPH: $FADH^-$-$NADP^+$ + NADPH ⇌ $FADH^-$-NADPH + $NADP^+$, where the $FADH^-$- NADPH complex does not exhibit significant charge transfer bands. This could be caused by a decrease in π−π stacking interactions between reduced FAD and NADPH. The value of $E_{ox/red}$ measured using dithionite as a reductant is −377 mV [32], which is fitted to a Nernstian n = 2 curve. However, the two-electron reduction potential in the presence of $NADP^+$ is divided into $E_{ox/sq}$ (−306 mV) and $E_{sq/red}$ (−386 mV) (**Table 1**), suggesting that the redox potentials of FNR are regulated by the $NADP^+$/NADPH ratio.

Table 1. Midpoint reduction potentials of FAD and FMN domains.

Enzyme Specicies	$E_{ox/sq}$ (mV)	$E_{sq/red}$ (mV)	pH
FNR (FAD)			
Spinach (FAD)	−350	−335	7
	−402	−358	8
Spinach (FAD)	−306	−386	8
(in the presence of $NADP^+$)			
Anabaena (FAD)	−385	−371	8
Anabaena Flavodoxin (FMN)	−212	−436	7
Cyt P450 reductase (FAD-FMN)			
Rabbit (FAD)	−290	−365	7
Rabbit (FMN)	−110	−270	7
Human (FAD)	−283	−382	7
Human (FMN)	−56	−274	7
nNOS reductase domain (FAD-FMN)			
Rat (FAD)	−260	−280	7.6
Rat (FMN)	−50	−276	7.6
iNOSreductase domain (FAD-FMN)			

Enzyme Specicies	$E_{ox/sq}$ (mV)	$E_{sq/red}$ (mV)	pH
Human (FAD)	−240	−270	7
Human (FMN)	−105	−245	7

and two-). For the oxidized-semiquinone couple ($E_{ox/sq}$) is −350 mV, and the semiquinone-fully reduced couple ($E_{sq/red}$) is −335 mV at pH 7.0 [34] (**Table 1**). Thus, the electron transfer from Fd I to $NADP^+$ is thermodynamically favorable. On the other hand, the electron transfer from NADPH to Fd III is relatively favorable. In both systems, tissue-specific FNR mediates reversible electron transfer reactions (Equation (1) and Scheme 1) [33].

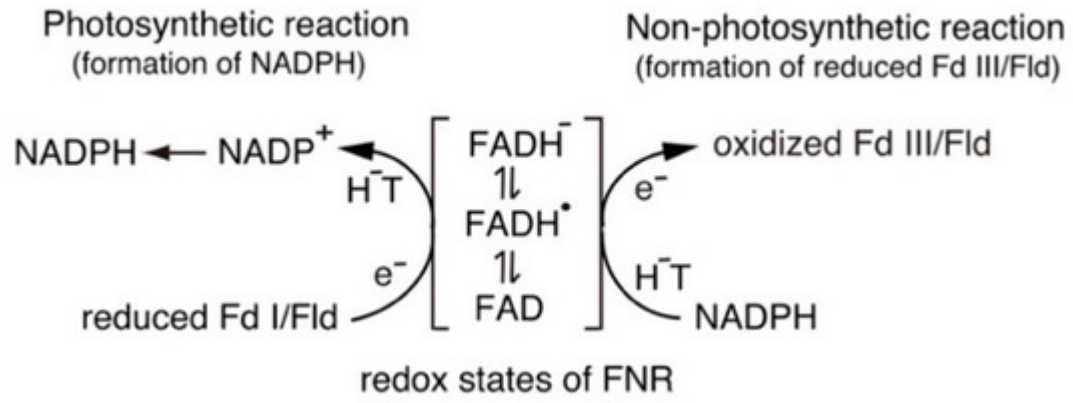

Scheme 1. Switching between one-electron and two-electron transfer reactions in the FNR-Fd I/Fld and FNR-Fd III/Fld systems. H^-T, hydride transfer.

Fld is a small electron carrier that participates in low-redox-potential electron transfer pathways, which are classified into three groups based on the presence of tryptophan (Trp) and tyrosine (Tyr) near the isoalloxazine ring of FMN [35]. In all Flds, the semiquinone formation constant *K*s value is larger than unity, indicating that the $E_{ox/sq}$ value is always more positive than the $E_{sq/red}$ value [36]. The $E_{ox/sq}$ value is associated with the proton-coupled one-electron reduction from FMN to $FMNH^•$, while $E_{sq/red}$ is associated with the one-electron reduction from $FMNH^•$ to $FMNH^-$. The $E_{ox/sq}$ value is shifted from ~−240 mV to less-than-negative values, while $E_{sq/red}$ is shifted from ~−170 mV to ~−540 mV, depending on the pH and the species of Fld. The neutral semiquinone, $FMNH^•$, is stabilized by the hydrogen bond of the carbonyl and amide groups of the protein backbone with the N5 atom of the isoalloxazine ring of the flavins. Its reactivity is lower than that of the fully reduced form, where the $FMNH^•/FMNH^-$ couple acts as a one-electron carrier [36].

Flds possess a unique structure, and the loop structures in the FMN environment play an important role in electron transfer reactions [37]. The FMN binding sites in the bacterial Fld and eukaryotic diflavin reductase family possess similar loop structures and are sandwiched between two aromatic amino acid residues. Rwere et al. [38] reported that the length and sequence of the “140 s” FMN binding loop of cyt P450 reductase functions as a key determinant of its redox potential and activity with cyt P450s. The one-electron redox potentials of cyt P450 reductase (FAD-FMN) [39][40] and the reductase domain (FAD-FMN) of NOS isoforms [41][42] are different from those of plant FNR (FAD) [34] and *Anabaena* flavodoxin (FMN) [43], but the one-electron redox potentials of FAD and FMN always satisfy $E_{ox/sq} > E_{sq/red}$ (Ref. [14] and **Table 1**).

The kinetic parameters for Fd reduction by FNR using the NADPH-dependent cyt *c* reductase assay (NADPH → FNR → Fd/Fld → cyt *c*) were reported [29]. The values for pea FNR are in the range of those of the *Anabaena* enzyme, with a slightly larger k_{cat} and a smaller K_m (**Table 2**) [29], while Kimata-Ariga and co-workers recently reported the tissue-specific parameters, where maize *R*FNR has a higher K_m value for Fd I than for Fd III [1]. In addition, the orientation of the *R*FNR-Fd complex remarkably varies from that of the *L*FNR-Fd complex [1], suggesting that the root and leaf complexes utilize the different sides of the [2Fe-2S] cluster for the intermolecular electron transfer, which might lead to the evolutional switch between photosynthetic and heterotrophic assimilation.

Table 2. Kinetic parameter of *Pea* and *Anabaena* FNR in NADPH-dependent cytochrome *c* reductase activity.

FNR Species	KFdcat (s−1)	KFdm **(μM)**	KFdcat/KFdm **(μM s^{-1})**	KFldcat (s−1)	KFldm **(μM)**	KFldcat/KFldm **(μM s^{-1})**
Pea FNR	139	6.5	21.3	30.6	16.7	1.8
Anabaena FNR	200	11	18.2	23.3	33	0.7

3. Catalytic Cycle of the FNR-Fd and FNR-Fld Systems

3.1. Catalytic Cycle of the FNR-Fd System

As already mentioned, the distinct isoforms of FNR and Fd are expressed in the different tissues, where *L*FNR and *L*Fd I are expressed in photosynthetic tissue, while *R*FNR and *R*Fd III are expressed in non-photosynthetic tissues. FNR mediates a switching between one-electron and two-electron transfer reactions (Scheme 1). Thus, the tissue-specific expression of the FNR and Fd isoforms indicates that different FNR and Fd isoforms participate in the different catalytic electron transfer processes (see **Figure 1**A,B). *L*FNR catalyzes the reduction of $NADP^+$ to NADPH during the photosynthetic process in plants and cyanobacteria, where the two electrons from photosystem I are transferred from $FADH^-$ to $NADP^+$ in a process defined by: photosystem I (PSI) → Fd I [2Fe-2S] (−401 mV) → *L*FNR (FAD) → $NADP^+$ (−320 mV). In non-photosynthetic reactions, NADPH generated by the photosynthetic reaction and the oxidative pentose phosphate cycle donates electrons to *R*Fd: NADPH (−320 mV) → *R*FNR (FAD) → Fd III (−321 mV) [33]. Thus, the photosynthetic process is more favorable than non-photosynthetic reactions. Both mechanisms are controlled by several factors: the redox potentials, the association/dissociation of complexes, and the distance between Fd [2Fe-2S] and FNR (FAD) in protein–protein interactions.

In photosystem I, the electron transfer sequence of the physiological reaction center is {P700* → A_o → A_1 → FeS-X → [FeS-A → FeS-B]} → Fd I, in which Fd I accepts an electron from the [FeS-B] site (−580 mV), and the resulting reduced Fd I (−401 mV) binds to the oxidized FNR (FAD_{ox}) [44], as shown in **Figure 1**A. Thus, Fd I functions as a mobile electron carrier. On the other hand, non-photosynthetic reactions begin from NADPH binding to the FAD_{ox}-Fd III_{ox} complex: NADPH → *R*FNR (FAD)-*R*Fd III, as shown in **Figure 1**B.

In 1984, Batie and Kamin [45] proposed the catalytic cycle of the *L*FNR and *L*Fd I system (**Figure 1**A). This cycle involves basic electron transfer reactions, including one-electron transfer ($1e^-$T), proton-coupled one-electron

transfer (PC1e$^-$T) and two-electron hydride transfer (H$^-$T) reactions. The catalytic cycle includes steps 1–7, where the catalytic cycle begins from *L*FNR (FAD_{ox}) (step 1). The oxidized Fd I accepts an electron from Photosystem I, and the resulting Fd I_{red} binds to the *L*FNR (FAD_{ox})-$NADP^+$ complex (step 2). One electron is then transferred from Fd I_{red} to *L*FNR (FAD_{ox}). In step 3, the one-electron transfer from reduced Fd I to oxidized FAD is coupled with proton transfer (PC1e$^-$T). Electron transfer in this step is significantly decreased in D_2O solution. In step 4, the Fd I_{ox} of the *L*FNR ($FADH^•$)-$NADP^+$ complex is replaced by reduced Fd I_{red}, thus resulting in the Fd I_{red}-*L*FNR ($FADH^•$)-$NADP^+$ complex. In step 5, the Fd_{ox}-*L*FNR($FADH^-$)-$NADP^+$ complex is formed via a one-electron transfer reaction (1e$^-$T) from Fd I_{red} to *L*FNR ($FADH^•$). In step 6, $NADP^+$ accepts a hydride from $FADH^-$ to form NADPH. In the final step, both Fd I_{ox} and NADPH are released; a new cycle then begins. This catalytic cycle is also supported by kinetic studies [46].

In 2003, Carrillo and Ceccarelli [47] proposed the “open questions” in regard to the Batie-Kamin catalytic model [45] on the basis of kinetics and binding experiments on spinach FNR. Currently, new data in regard to these open questions can be found (see Refs [1][48][49][50]).

In non-photosynthetic reactions (metabolic redox pathways) (**Figure 1**B), the reaction begins with *R*FNR (FAD_{ox}). In the first step, NADPH binds to the FAD_{ox}-Fd III_{ox} complex. In step 2, the complex $NADP^+$-$FADH^-$-Fd III_{ox} is formed via the hydride transfer (H$^-$T) reaction, and this complex is followed by the formation of the $NADP^+$-FNR ($FADH^•$)-Fd III_{red} complex via one-electron transfer (1e$^-$T) from $FADH^-$ to Fd III_{ox} (step 3). In step 4, Fd III_{red} is released from the complex, and Fd III_{ox} binds. In step 5, the $NADP^+$-FNR (FAD_{ox})-Fd III_{red} complex is formed via PC1e$^-$T. In the final step, Fd III_{red} and $NADP^+$ are released. Thus, reduced Fd III is formed in steps 3 and 5.

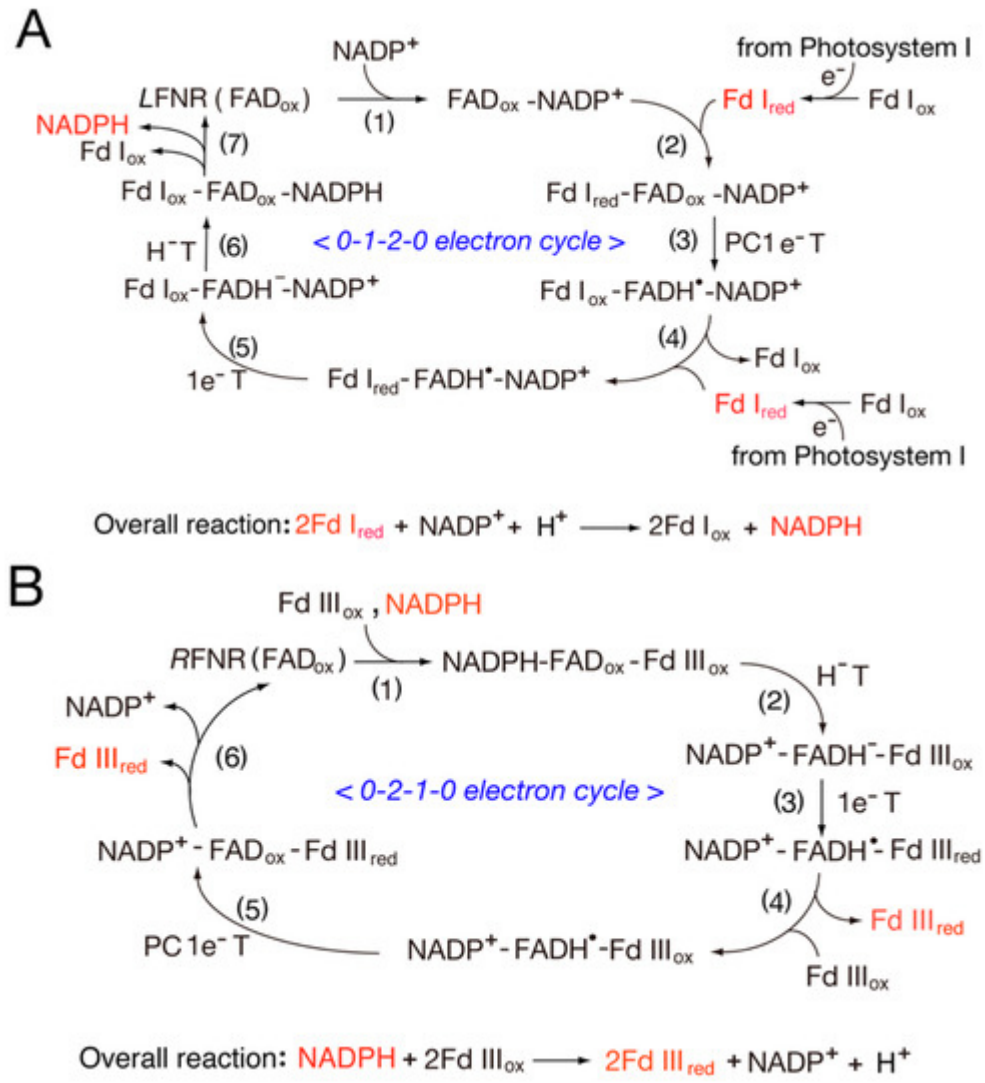

Figure 1. Proposed catalytic cycles of the *L*FNR (**A**) and *R*FNR (**B**) systems. (**A**) Photosystem I → *L*Fd I (2S-2Fe) → *L*FNR (FAD) → $NADP^+$ [45] and (**B**) NADPH→*R*FNR (FAD) → *R*Fd III→metabolic pathways. H^-T, hydride transfer; $1e^-T$, one-electron transfer; $PC1e^-T$, proton-coupled one-electron transfer.

3.2. Catalytic Cycle of the FNR-Fld Systems

Fd can be replaced with FMN-containing Fld, where the FNR-Fd pair is replaced with the FNR-Fld pair in the catalytic cycle (**Figure 2**A). The FMN semiquinone ($FMNH^•$) is highly stable. Thus, Fld functions as a one-electron carrier ($FMNH^- \rightleftharpoons FMNH^• + e^-$). In the photosynthetic process, the catalytic cycle (**Figure 2**A) is similar to that presented in **Figure 1**A.

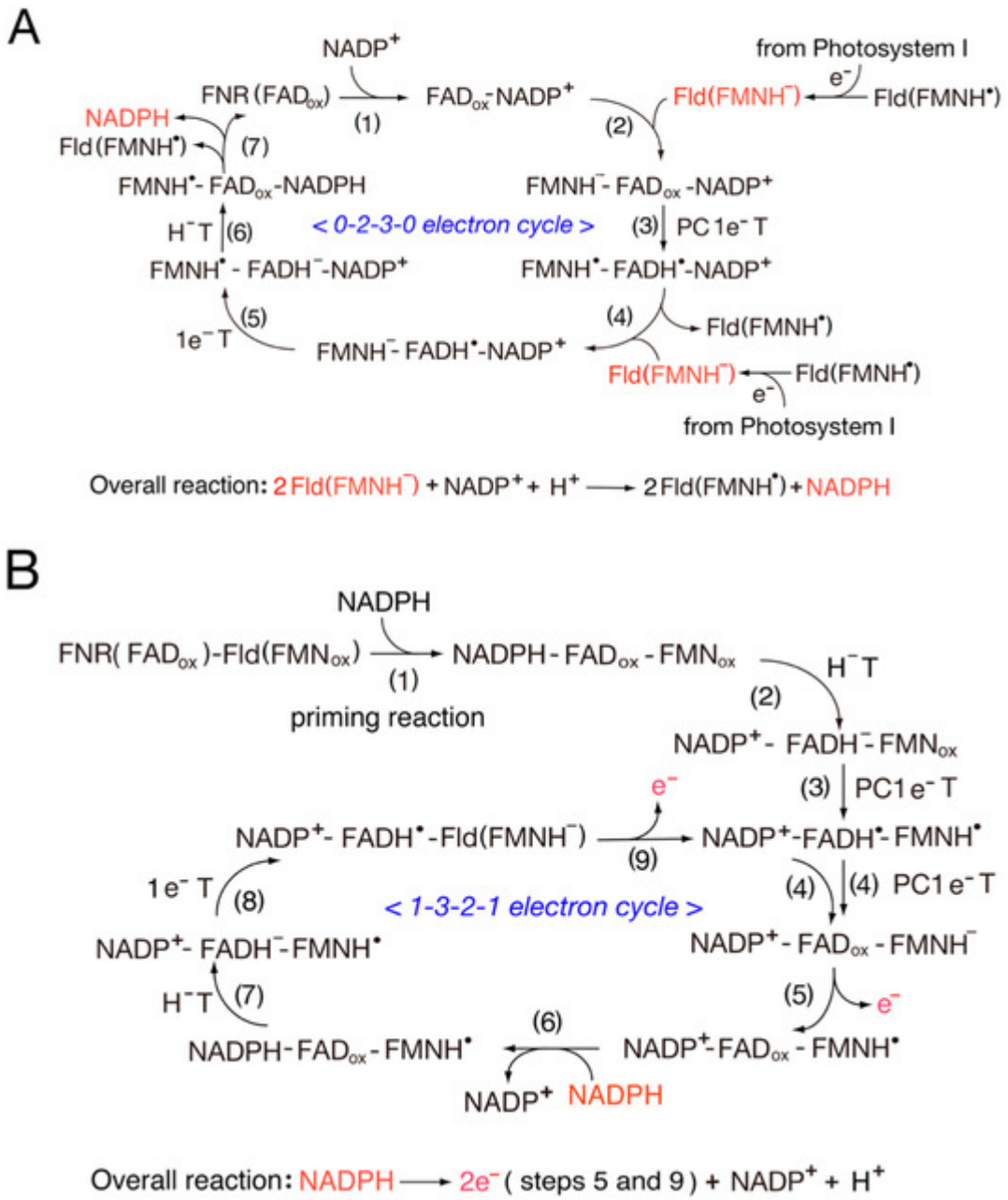

Figure 2. Proposed catalytic cycle of the FNR-Fld systems. (**A**) Photosystem I → Fld (FMN) → FNR (FAD) → $NADP^+$ and (**B**) NADPH → FNR (FAD) → Fld (FMN) → metabolic redox pathways. In (**B**), the overall reaction is based on the catalytic cycle.

In the first step, $NADP^+$ binds to *L*FNR (FAD_{ox}). In step 2, reduced Fld ($FMNH^-$) binds to FNR (FAD_{ox})-$NADP^+$, and in step 3, the diflavin radical intermediate $FMNH^•$-$FADH^•$-$NADP^+$ is formed via a PC1e^-T reaction. Such intermediates are observed in the *Anabaena* PSI/Fld system [51]. In step 4, Fld ($FMNH^•$) releases, and Fld ($FMNH^-$) binds. In step 5, $FMNH^•$-$FADH^-$-$NADP^+$ is formed during a 1e^-T reaction, and in step 6, $FMNH^•$-FAD_{ox}-NADPH is formed during an H^-T reaction. In the final step, Fld ($FMNH^•$) and NADPH are released.

The catalytic cycle of the non-photosystem includes the priming reaction (**Figure 2**B). The catalytic cycle begins from the complex $NADP^+$-FAD_{ox}-$FMNH^•$ and includes the following sequences: (6) → (7) → (8) → (9) → (4) → (5),

where the catalytic cycle shuttles among the 1-3-2-1 electron reduced states. The two electrons from steps 5 and 9 are transferred to the metabolic redox pathways. This overall catalytic cycle is very similar to that of cyt P450 reductase (see **Figure 3**), where the diflavin radical intermediate, FADH•-FMNH•, is formed through the catalytic cycle (step 9).

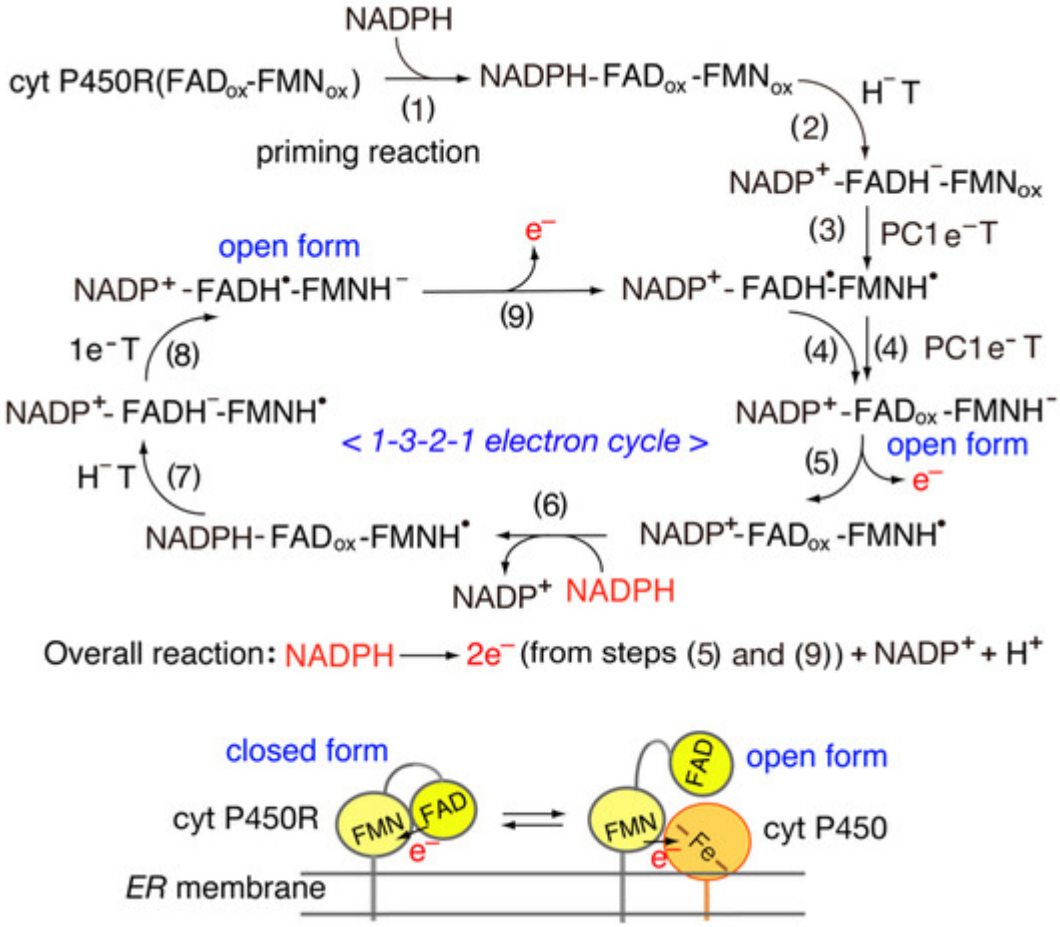

Figure 3. Proposed catalytic cycle of the eukaryotic-membrane-bound cyt P450 reductase-cyt P450 system. In this figure, the overall reaction is based on the catalytic cycle. Note that cyt P450R indicates cyt P450 reductase. $H^{-}T$, hydride transfer; $1e^{-}T$, one-electron transfer; $PC1e^{-}$ T, proton-coupled one-electron transfer.

Recently, Utschig et al. [52] proposed a new approach for the electron transfer from photosystem I to Fd I/Fld in which Fd I and Fld are covalently bound by a ruthenium photosensitizer (RuPS) instead of photosystem I. The RuPS is activated by light, whereby an electron is transferred from activated RuPS*: RuPS*-Fd I → FNR and RuPS*-Fld → FNR, respectively. In these cases, an electron transfer occurs within the Fd I/Fld and FNR complexes. In both cases, FNR semiquinone intermediates are observed using electron-spin resonance. In the final step, oxidized $NADP^{+}$ accepts hydride from $FADH^{-}$. This report suggests that photosystem I could sequentially donate one electron to the oxidized Fd I/Fld-oxidized FNR complexes. The electron transfer mechanisms are different from those of **Figure 1**A and **Figure 2**A, but this new approach could provide an excellent model system for photosystem I.

4. Structure and Properties of Diflavin Reductase Family

The electron transfer cascade catalyzed by FNR is arranged as presented in Scheme 2. FNR selects a one-electron carrier as a partner of electron transfer systems in which three components, iron sulfur protein ferredoxin, FMN-containing flavodoxin and heme-containing cytochromes, function as a one-electron carrier. Thus, at least three different electron transfer systems might be diversified during the processes of evolution.

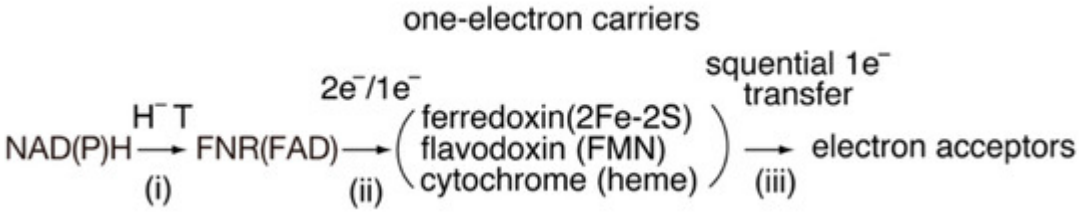

Scheme 2. The roles of FNR (FAD) and one-electron carriers in the NAD(P)H-dependent electron transfer systems.

The eukaryotic FAD- and FMN-containing diflavin reductase family members are fusion enzymes in which the structure of the FAD/NADPH-binding C-terminal domain is structurally homologous to that of plant FNR, while the FMN-binding N-terminal domain is similar to that of bacterial FMN-containing flavodoxin (Fld). Furthermore, cyt P450 reductase [40][53], methionine synthase (MS) reductase (MS reductase) [54][55], novel reductase 1 (NR1) [56], sulfite reductase (SiR) [57] and P450BM3 [58] are members of the diflavin oxidoreductase family, where the distinct FAD and FMN domains are connected by an additional connecting domain (CD) and flexible hinge (H) [59].

The catalytic cycle of cyt P450 reductase as a prototypic member of the diflavin reductase family is very similar to that of the catalytic cycle of the non-photosystem FNR-Fld system (**Figure 3**). The catalytic cycle of the membrane-bound type is closely related to that presented in **Figure 2**B. However, the intermolecular electron transfer between FAD and FMN occurs in the closed form, while its open form donates electrons to cyt P450s in a stepwise manner [12]. On one hand, cyt P450 catalyzes the consumption of one molecule of oxygen/molecule of substrate (RH); one atom of this oxygen molecule inserts into the product (ROH), and the other undergoes two equivalents of reduction: $RH + 2e^- + O_2 + 2H^+ \rightarrow ROH + H_2O$. On the other hand, methionine synthase (MS) reductase [55] and novel reductase 1 (NR1) [56] are soluble forms that lack the N-terminal anchors domain. For these enzymes, the catalytic cycle is similar to that of the membrane-bound form [14].

In contrast, the reductase domain of NOS isoforms contains additional regulatory elements within the C-terminal reductase domain that control the electron transfer through Ca^{2+}-dependent calmodulin (CaM) binding [12][14][60]. The mechanism of FAD reduction by NADPH is closely related to that of mammalian cyt P450 reductase. However, the neuronal (nNOS) and endotherial (eNOS) isoforms are activated by Ca^{2+}/CaM binding [60]. On the other hand, the inducible (iNOS) isoform tightly binds Ca^{2+}/CaM, and iNOS activity is independent of intracellular Ca^{2+} concentrations. Thus, the iNOS isoform is likely to have functions and mechanism similar to those of cyt 450 reductase [60].

References

1. Shinohara, F.; Kurisu, G.; Hanke, G.; Bowsher, C.; Hase, T.; Kimata-Ariga, Y. Structural basis for the isotype-specific interactions of ferredoxin and ferredoxin: NADP+ oxidoreductase: An evolutionary switch between photosynthetic and heterotrophic assimilation. Photosynth. Res. 2017, 134, 281–289.
2. Hanke, G.T.; Kurisu, G.; Kusunoki, M.; Hase, T. Fd: FNR electron transfer complexes: Evolutionary refinement of structural interactions. Photosynth. Res. 2004, 81, 317–327.
3. Ceccarelli, E.A.; Arakaki, A.K.; Cortez, N.; Carrillo, N. Functional plasticity and catalytic efficiency in plant and bacterial ferredoxin-NADP (H) reductases. Biochim. Biophys. Acta Proteins Proteom. 2004, 1698, 155–165.
4. Aliverti, A.; Pandini, V.; Pennati, A.; de Rosa, M.; Zanetti, G. Structural and functional diversity of ferredoxin-NADP+ reductases. Arch. Biochem. Biophys. 2008, 474, 283–291.
5. Karplus, P.A.; Daniels, M.J. Atomic structure of ferredoxin-NADP+ reductase: Prototype for a structurally novel flavoenzyme family. Science 1991, 251, 60–66.
6. Sánchez-Azqueta, A.; Catalano-Dupuy, D.L.; López-Rivero, A.; Tondo, M.L.; Orellano, E.G.; Ceccarelli, E.A.; Medina, M. Dynamics of the active site architecture in plant-type ferredoxin-NADP+ reductases catalytic complexes. Biochim. Biophys. Acta Bioenerg. 2014, 1837, 1730–1738.
7. Onda, Y.; Matsumura, T.; Kimata-Ariga, Y.; Sakakibara, H.; Sugiyama, T.; Hase, T. Differential interaction of maize root ferredoxin: NADP+ oxidoreductase with photosynthetic and non-photosynthetic ferredoxin isoproteins. Plant. Physiol. 2000, 123, 1037–1046.
8. Tognetti, V.B.; Zurbriggen, M.D.; Morandi, E.N.; Fillat, M.F.; Valle, E.M. Enhanced plant tolerance to iron starvation by functional substitution of chloroplast ferredoxin with a bacterial flavodoxin. Proc. Natl. Acad. Sci. USA 2007, 104, 11495–11500.
9. Porter, T.D.; Kasper, C.B. NADPH-cytochrome P-450 oxidoreductase: Flavin mononucleotide and flavin adenine dinucleotide domains evolved from different flavoproteins. Biochemistry 1986, 25, 1682–1687.
10. Haniu, M.; Iyanagi, T.; Miller, P.; Lee, T.D.; Shively, J.E. Complete amino acid sequence of NADPH-cytochrome P-450 reductase from porcine hepatic microsomes. Biochemistry 1986, 25, 7906–7911.
11. Bredt, D.S.; Hwang, P.M.; Glatt, C.E.; Lowenstein, C.; Reed, R.R.; Snyder, S.H. Cloned and expressed nitric oxide synthase structurally resembles cytochrome P-450 reductase. Nature 1991, 351, 714–718.

12. Iyanagi, T.; Xia, C.; Kim, J.J. NADPH-cytochrome P450 oxidoreductase: Prototypic member of the diflavin reductase family. Arch. Biochem. Biophys. 2012, 528, 72–89.
13. Ingelman, M.; Bianchi, V.; Eklund, H. The three-dimensional structure of flavodoxin reductase from Escherichia coli at 1.7 Å resolution. J. Mol. Biol. 1997, 268, 147–157.
14. Iyanagi, T. Molecular mechanism of metabolic NAD(P)H-dependent systems: The role of redox cofactors. Biochim. Biophys. Acta Bioenerg. 2019, 1860, 233–258.
15. Iyanagi, T.; Yamazaki, I. One-electron-transfer reactions in biochemical systems III. One-electron reduction of quinones by microsomal flavin enzymes. Biochim. Biophys. Acta Bioenerg. 1969, 172, 370–381.
16. Iyanagi, T.; Yamazaki, I. One-electron-transfer reactions in biochemical systems V. Difference in the mechanism of quinone reduction by the NADH dehydrogenase and the NAD (P) H dehydrogenase (DT-diaphorase). Biochim. Biophys. Acta Bioenerg. 1970, 216, 282–294.
17. Čenas, N.; Anusevičius, Ž.; Bironaite, D.; Bachmanova, G.I.; Archakov, A.I.; Öllinger, K. The electron transfer reactions of NADPH: Cytochrome P450 reductase with nonphysiological oxidants. Arch. Biochem. Biophys. 1994, 315, 400–406.
18. Čenas, N.; Anusevičius, Ž.; Nivinskas, H.; Misevičienė, L.; Šarlauskas, J. Structure-Activity Relationships in Two-Electron Reduction of Quinones. Methods Enzym. B. 2004, 382, 258–277.
19. Anusevičius, Ž.; Misevičienė, L.; Medina, M.; Martinez-Julvez, M.; Gomez- Moreno, C.; Čėnas, N. FAD semiquinone stability regulates single-and two-electron reduction of quinones by Anabaena PCC7119 ferredoxin: NADP+ reductase and its Glu301Ala mutant. Arch. Biochem. Biophys. 2005, 437, 144–150.
20. Bianchet, M.A.; Faig, M.; Amzel, L.M. Structure and mechanism of NAD H: Quinone acceptor oxidoreductases (NQO). Methods Enzymol. 2004, 382, 144–174.
21. Iyanagi, T. Molecular mechanism of phase I and phase II drug-metabolizing enzymes: Implications for detoxification. Int. Rev. Cytol. 2007, 260, 35–112.
22. Martínez-Júlvez, M.; Medina, M.; Gómez-Moreno, C. Ferredoxin-NADP+ reductase uses the same site for the interaction with ferredoxin and flavodoxin. J. Biol. Chem. 1999, 4, 568–578.
23. Medina, M. Structural and mechanistic aspects of flavoproteins: Photosynthetic electron transfer from photosystem I to NADP+. FEBS J. 2009, 276, 3942–3958.
24. Kurisu, G.; Kusunoki, M.; Katoh, E.; Yamazaki, T.; Teshima, K.; Onda, Y.; Kimata-Ariga, Y.; Hase, T. Structure of the electron transfer complex between ferredoxin and ferredoxin-NADP+ reductase. Nat. Struct. Biol. 2002, 8, 117–121.
25. Medina, M.; Abagyan, R.; Gómez-Moreno, C.; Fernandez-Recio, J. Docking analysis of transient complexes: Interaction of ferredoxin-NADP+ reductase with ferredoxin and flavodoxin. Proteins

2008, 72, 848–862.

26. Chikuma, Y.; Miyata, M.; Lee, Y.H.; Hase, T.; Kimata-Ariga, Y. Molecular mechanism of negative cooperativity of ferredoxin-NADP+ reductase by ferredoxin and NADP (H): Involvement of a salt bridge between Asp60 of ferredoxin and Lys33 of FNR. Biosci. Biotechnol. Biochem. 2021, 85, 860–865.
27. Buchert, F.; Hamon, M.; Gäbelein, P.; Scholz, M.; Hippler, M.; Wollman, F.A. The labile interactions of cyclic electron flow effector proteins. J. Biol. Chem. 2018, 293, 17559–17573.
28. Kean, K.M.; Carpenter, R.A.; Pandini, V.; Zanetti, G.; Hall, A.R.; Faber, R.; Aliverti, A.; Karplus, P.A. High resolution studies of hydride transfer in the ferredoxin: NADP+ reductase superfamily. FEBS J. 2017, 284, 3302–3319.
29. Nogués, I.; Tejero, J.; Hurley, J.K.; Paladini, D.; Frago, S.; Tollin, G.; Mayhew, S.G.; Gomez-Moreno, G.; Eduardo, A.; Ceccarelli, E.A.; et al. Role of the C-terminal tyrosine of ferredoxin-nicotinamide adenine dinucleotide phosphate reductase in the electron transfer processes with its protein partners ferredoxin and flavodoxin. Biochemistry 2004, 43, 6127–6137.
30. Dumit, V.I.; Essigke, T.; Cortez, N.; Ullmann, G.M. Mechanistic insights into ferredoxin–NADP(H) reductase catalysis involving the conserved glutamate in the active site. J. Mol. Biol. 2010, 397, 814–825.
31. Faro, M.; Gómez-Moreno, C.; Stankovich, M.; Medina, M. Role of critical charged residues in reduction potential modulation of ferredoxin-NADP+ reductase: Differential stabilization of FAD redox forms. Eur. J. Biochem. 2002, 269, 2656–2661.
32. Batie, C.J.; Kamin, H. Association of ferredoxin-NADP+ reductase with NADP(H) specificity and oxidation-reduction properties. J. Biol. Chem. 1986, 261, 11214–11223.
33. Aliverti, A.; Faber, R.; Finnerty, C.M.; Ferioli, C.; Pandini, V.; Negri, A.; Karplus, P.A.; Zanetti, G. Biochemical and crystallographic characterization of Ferredoxin− NADP+ Reductase from nonphotosynthetic tissues. Biochemistry 2001, 40, 14501–14508.
34. Corrado, M.E.; Aliverti, A.; Zanetti, G.; Mayhew, S.G. Analysis of the oxidation-reduction potentials of recombinant ferredoxin-NADP+ reductase from spinach chloroplasts. Eur. J. Biochem. 1996, 239, 662–667.
35. Druhan, L.J.; Swenson, R.P. Role of Methionine 56 in the Control of the Oxidation−Reduction Potentials of the Clostridium beijerinckii Flavodoxin: Effects of Substitutions by Aliphatic Amino Acids and Evidence for a Role of Sulfur−Flavin Interactions. Biochemistry 1998, 37, 9668–9678.
36. Ishikita, H. Influence of the protein environment on the redox potentials of flavodoxins from Clostridium beijerinckii. J. Biol. Chem. 2007, 282, 25240–25246.

37. Chang, C.W.; He, T.F.; Guo, L.; Stevens, J.A.; Li, T.; Wang, L.; Zhong, D. Mapping solvation dynamics at the function site of flavodoxin in three redox states. J. Am. Chem. Soc. 2010, 132, 12741–12747.
38. Rwere, F.; Im, S.; Waskell, L. The FMN “140s Loop” of Cytochrome P450 Reductase Controls Electron Transfer to Cytochrome P450. Int. J. Mol. Sci. 2021, 22, 10625.
39. Iyanagi, T.; Makino, N.; Mason, H.S. Redox properties of the reduced nicotinamide adenine dinucleotide phosphate-cytochrome P-450 and reduced nicotinamide adenine dinucleotide-cytochrome b5 reductases. Biochemistry 1974, 13, 1701–1710.
40. Munro, A.W.; Noble, M.A.; Robledo, L.; Daff, S.N.; Chapman, S.K. Determination of the redox properties of human NADPH-cytochrome P450 reductase. Biochemistry 2001, 40, 1956–1963.
41. Haque, M.M.; Tejero, J.; Bayachou, M.; Kenney, C.T.; Stuehr, D.J. A cross-domain charge interaction governs the activity of NO synthase. J. Biol. Chem. 2018, 293, 4545–4554.
42. Gao, Y.T.; Smith, S.M.; Weinberg, J.B.; Montgomery, H.J.; Newman, E.; Guillemette, J.G.; Ghosh, D.K.; Roman, L.J.; Martasek, P.; Salerno, J.C. Thermodynamics of oxidation-reduction reactions in mammalian nitric-oxide synthase isoforms. J. Biol. Chem. 2004, 279, 18759–18766.
43. Pueyo, J.J.; Gomez-Moreno, C.; Mayhew, S.G. Oxidation-reduction potentials of ferredoxin-NADP+ reductase and flavodoxin. from Anabaena PCC 7119 and their electrostatic and covalent complexes. Eur. J. Biochem. 1991, 202, 1065–1071.
44. Diaz-Quintana, A.; Leibl, W.; Bottin, H.; Sétif, P. Electron transfer in photosystem I reaction centers follows a linear pathway in which iron-sulfur cluster FB is the immediate electron donor to soluble ferredoxin. Biochemistry 1998, 37, 3429–3439.
45. Batie, C.J.; Kamin, H. Electron transfer by ferredoxin: NADP+ reductase. Rapid -reaction evidence for participation of a ternary complex. J. Biol. Chem. 1984, 259, 11976–11985.
46. Walker, M.C.; Pueyo, J.; Navarro, J.; Gómez-Moreno, C.; Tollin, G. Laser flash photolysis studies of the kinetics of reduction of ferredoxins and ferredoxin-NADP+ reductases from Anabaena PCC 7119 and spinach: Electrostatic effects on intracomplex electron transfer. Arch. Biochem. Biophys. 1991, 287, 351–358.
47. Carrillo, N.; Ceccarelli, E.A. Open questions in ferredoxin-NADP+ reductase catalytic mechanism. Eur. J. Biochem. 2003, 270, 1900–1915.
48. Tejero, J.; Peregrina, J.R.; Martínez-Júlvez, M.; Gutiérrez, A.; Gomez-Moreno, C.; Scrutton, N.S.; Medina, M. Catalytic mechanism of hydride transfer between NADP+/H and ferredoxin-NADP+ reductase from Anabaena PCC 7119. Arch. Biochem. Biophys. 2007, 459, 79–90.
49. Mulo, P.; Medina, M. Interaction and electron transfer between ferredoxin–NADP+ oxidoreductase and its partners: Structural, functional, and physiological implications. Photosynth. Res. 2017,

134, 265–280.

50. Saen-Oon, S.; de Vaca, I.C.; Masone, D.; Medina, M.; Guallar, V. A theoretical multiscale treatment of protein–protein electron transfer: The ferredoxin/ ferredoxin-NADP+ reductase and flavodoxin/ferredoxin-NADP+ reductase systems. Biochim. Biophys. Acta Bioenerg. 2015, 1847, 1530–1538.
51. Nogués, I.; Martínez-Júlvez, M.; Navarro, J.A.; Hervás, M.; Armenteros, L.; de la Rosa, M.A.; Brodie, T.B.; Hurley, J.K.; Tollin, G.; Gomez-Moreno, C.; et al. Role of hydrophobic interactions in the flavodoxin mediated electron transfer from photosystem I to ferredoxin-NADP+ reductase in Anabaena PCC 7119. Biochemistry 2003, 42, 2036–2045.
52. Utschig, L.M.; Brahmachari, U.; Mulfort, K.L.; Niklas, J.; Poluektov, O.G. Biohybrid photosynthetic charge accumulation detected by flavin semiquinone formation in ferredoxin-NADP+ reductase. Chem. Sci. 2022, 12, 6502–6511.
53. Iyanagi, T.; Mason, H.S. Properties of hepatic reduced nicotinamide adenine dinucleotide phosphate-cytochrome c reductase. Biochemistry 1973, 12, 2297–2308.
54. Leclerc, D.; Wilson, A.; Dumas, R.; Gafuik, C.; Song, D.; Watkins, D.; Heng, H.H.; Rommens, J.M.; Scherer, S.W.; Rosenblatt, D.S.; et al. Cloning and mapping of a cDNA for methionine synthase reductase, a flavoprotein defective in patients with homocystinuria. Proc. Natl. Acad. Sci. USA 1998, 95, 3059–3064.
55. Wolthers, K.R.; Scrutton, N.S. Cobalamin uptake and reactivation occurs through specific protein interactions in the methionine synthase–methionine synthase reductase complex. FEBS J. 2009, 276, 1942–1951.
56. Paine, M.J.; Garner, A.P.; Powell, D.; Sibbald, J.; Sales, M.; Pratt, N.; Smith, T.; Tew, D.G.; Wolf, C.R. Cloning and characterization of a novel human dual flavin reductase. J. Biol. Chem. 2000, 275, 1471–1478.
57. Ostrowski, J.; Barber, M.J.; Rueger, D.C.; Miller, B.E.; Siegel, L.M.; Kredich, N.M. Characterization of the flavoprotein moieties of NADPH-sulfite reductase from Salmonella typhimurium and Escherichia coli. Physicochemical and catalytic properties, amino acid sequence deduced from DNA sequence of cysJ, and comparison with NADPH-cytochrome P-450 reductase. J. Biol. Chem. 1989, 264, 15796–15808.
58. Narhi, L.O.; Fulco, A.J. Characterization of a catalytically self-sufficient 119,000-dalton cytochrome P-450 monooxygenase induced by barbiturates in Bacillus megaterium. J. Biol. Chem. 1986, 261, 7160–7169.
59. Wang, M.; Roberts, D.L.; Paschke, R.; Shea, T.M.; Masters, B.S.S.; Kim, J.J.P. Three-dimensional structure of NADPH–cytochrome P450 reductase: Prototype for FMN-and FAD-containing enzymes. Proc. Natl. Acad. Sci. USA 1997, 94, 8411–8416.

60. Xia, C.; Misra, I.; Iyanagi, T.; Kim, J.J.P. Regulation of interdomain interactions by calmodulin in inducible nitric-oxide synthase. J. Biol. Chem. 2009, 284, 30708–30717.